# Significance of High-Pressure-Torsion Processing on an Aluminum-Lithium Aerospace Alloy

by
Marina Keller

A THESIS

submitted to

Oregon State University

Honors College

In partial fulfillment of
the requirements for the
degree of

Honors Baccalaureate of Science in Mechanical Engineering
Honors Scholar

Presented May 24, 2022
Commencement June, 2022

AN ABSTRACT OF THE THESIS OF

Marina Keller for the degree of Honors Baccalaureate of Science in Mechanical Engineering presented on May 24, 2022. Title: Significance of High-Pressure-Torsion Processing on an Aluminum-Lithium Aerospace Alloy

Abstract Approved:_____
Megumi Kawasaki

Aluminum alloys are popular in aerospace and automotive industries because of their relatively high strength-to-weight ratio. The study of enhancing aluminum's mechanical properties through grain refinement is especially important. One such technique is High-Pressure Torsion processing (HPT), which leads to significant grain size refinement and enhances mechanical properties like ductility and strength. Although an increase in material strength usually results in loss of ductility, severe plastic deformation has the ability to maintain both desirable properties. In the present study, the principle of HPT was applied to an aerospace grade Aluminum-Lithium alloy, Al-2099, under a compressive pressure of 6.0 GPa and a rotational speed of 1 rpm for up to 20 rotations at room temperature. The development of the alloy's microstructure is observed by X-ray diffraction analysis, while the development of microstructural heterogeneity was studied with hardness measurements. This study demonstrates the relationship between HPT processing, grain-size refinement, and enhanced mechanical properties. By studying this relationship, this study underscores the importance of severe plastic deformation for those seeking to drastically enhance metallic mechanical properties.

Significance of High-Pressure-Torsion Processing on an Aluminum-Lithium Aerospace Alloy

by
Marina Keller

A THESIS

submitted to

Oregon State University

Honors College

In partial fulfillment of
the requirements for the
degree of

Honors Baccalaureate of Science in Mechanical Engineering
Honors Scholar

Presented May 24, 2022
Commencement June, 2022

Honors Baccalaureate of Science in Mechanical Engineering of Marina Keller presented on May 24, 2022

APPROVED:

_____

Megumi Kawasaki, representing Material Science

_____

Deborah Pence, Committee Member, representing Mechanical Engineering

_____

Julie Tucker, Committee Member, representing Materials Science

_____

Toni Doolen, Dean, Oregon State University Honors College

I understand that my project will become part of the permanent collection of Oregon State University, Honors College. My signature below authorizes release of my project to any reader upon request.

_____

Marina Keller, Author

Table of Contents

# 1. Introduction

Aluminum alloys are of vital importance to manufacturing industries due to their relatively high strength, abundance in nature, and low density. These properties are particularly important for aerospace and automotive industries, as a lightweight and affordable material further lowers the cost of transportation and shipping. In addition, aluminum is widely available through both commercial and engineering markets [1]. Advancements in processing techniques mean that aluminum's mechanical properties can be enhanced. These desirable properties have drawn attention from aerospace and automotive industries, which are seeking materials with improved strength, corrosion resistance, and ductility.

Aluminum has a face centered cubic crystal structure, which enables dislocations to form along the most dense family planes of (111) and slip along the <110> family directions. Face centered cubic structures lend themselves well to plastic deformation along these densely packed planes, which results in a relatively ductile and malleable metal. This, however, means that face centered cubic aluminum alloys are not as strong as some other commercially available metals, such as steel.

The tradeoff between ductility and strength is understandably of great interest to researchers and industries. Many studies have discovered various processes by which one can improve the strength of a metal without sacrificing ductility. These techniques mainly focus on grain size refinement through accessible processes like cold rolling. The most common of these techniques include strain hardening, precipitation hardening, and solid solution strengthening. However, there is a limit to how much these mechanical properties can be improved through material processing. After a certain amount of grain size refinement, the material will become saturated with dislocations and the grain size cannot be refined anymore.

In addition, it is ideal to refine these metals at room temperature from a cost-standpoint. This is due to the fact that high-temperature processing is expensive and has a long processing time. This is where severe plastic deformation (SPD) techniques come into play, as they can achieve incredible grain refinement at room temperature.

SPD produces homogenous grain refinement and a unique paradox: the metal is both strong and ductile, which are two properties which rarely occur at the same time in a metal. This preservation of ductility occurs because SPD techniques introduce non-equilibrium grain boundaries [2] which have the ability to absorb numerous dislocations during processing, leading

to strain hardening and thereby exhibiting excellent strength and ductility. Out of the numerous SPD techniques, High-Pressure Torsion (HPT), is widely considered the most effective. This method applies highly compressive pressure and torsional stress to the material. These two loading methods induce dislocations within the material, and result in ultra-fine grained microstructures with both superior strength and enhanced ductility.

In the present study, aerospace-grade Aluminum-Lithium alloy, Al-2099, disks are processed via HPT under a compressive pressure of 6.0 GPa for up to 20 turns with a speed of 1 r.p.m. at room temperature. The development of Al-2099's microstructure is observed through X-Ray diffraction, and the development of hardness is studied through hardness measurements. This study ultimately demonstrates the relationship between HPT processing, grain refinement, and enhanced mechanical properties.

# 2. Literature Review

## 2.1 Ultrafine Grained Materials

Significant effort has gone into researching methods by which grain sizes can be further reduced in bulk metals. This effort is important because smaller grain sizes are associated with attractive mechanical properties, such as enhanced hardness, ductility, and wear resistance [3].

Many of these efforts have occurred in the past three decades, where the conventional metal processes such as extrusion and cold rolling were being used to achieve some of these refined microstructures. While ultrafine grained materials are classified by grain sizes of 100-1000 nm, there is an effort to further refine the microstructure within a range of 10 to 100 nm. Achieving this desirable nanocrystalline microstructure requires specialized processing techniques.

One promising technique is the top-down approach. This technique subjects bulk materials to intense hydrostatic pressures and induces high concentrations of dislocations and lattice defects. Due to the high pressures, one can process bulk materials into desirable, ultrafine grained materials [4,5].

Understanding the relationship between microstructure and strength is extremely important. The Hall-Petch relationship (Equation 2.1) relates a material's yield strength, $\sigma_y$, to

the average grain size, *d,* where $k_y$ is the yielding constant and $\sigma_0$ is the lattice friction stress [6,7].

$$\sigma_y = \sigma_0 + k_y d^{-1/2} \qquad \text{Equation 2.1}$$

This relationship indicates that a smaller average grain size will increase the yield strength of a material. However when the material is subjected to temperatures higher than half of its melting point, the relationship becomes less accurate [8]. This increase in heat, stored within the material, affects the mechanical properties of the metal.This is because high thermal energy stores, although advantageous in increasing metallic ductility, ultimately lower the strength of a material through recrystallization. Slip along the grain boundaries (known as GBS, grain boundary slip) occurs more readily at high temperatures, so the Hall-Petch equation cannot accurately describe the strength-to-diameter relationship at elevated temperatures [9].

Numerous studies have attempted to enhance both the ductility and strength of a material. This, however, is incredibly difficult to realize as an increase in strength is almost always a result of a decrease in ductility [10]. This phenomenon is known as *the paradox of strength and ductility*, where most metals have either incredible ductility *or* strength, almost never both [11]. This paradox can be visualized in Figure 2.1, where many common metallic materials which fit in the gray region behave strong but less ductile or demonstrate high elongation to failure but low strength.

Achieving this paradox of high strength and good ductility requires material processing techniques such as HPT, which subject a material to incredibly large strains under hydrostatic pressure. In Figure 2.1, one can see two interesting outliers of metals that have both strength and ductility: nano Ti and nano Cu. Both of these metallic materials were subjected to severe plastic deformation processing prior to testing, whereas none of the other metals were.

This figure indicates that severe plastic deformation processing enhances both the ductility and the strength of metallic compounds. By subjecting metals to extremely large strains, one can develop an ultrafine grained material with superior mechanical properties [12].

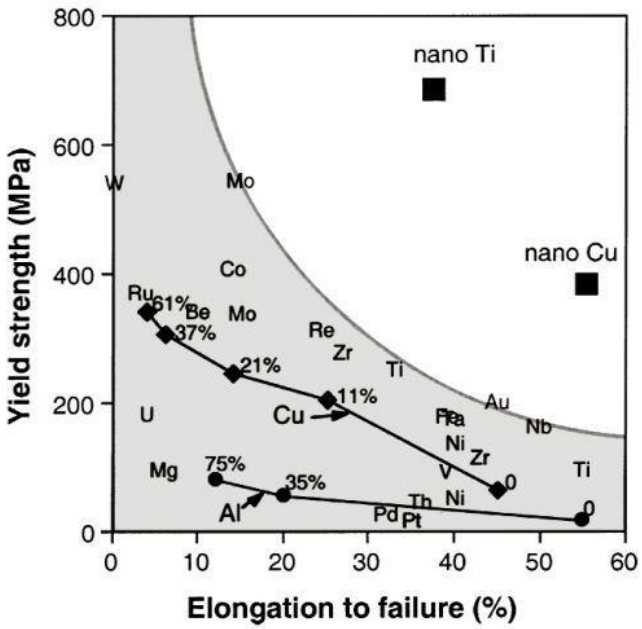


*Figure 2.1 Yield Stress as a function of elongation to failure. This figure demonstrates the tradeoff between a material's ductility and strength, as well as the importance of HPT processing [11]*

As the average grain size of a material decreases, the strength, toughness and ductility all see significant improvement [13].

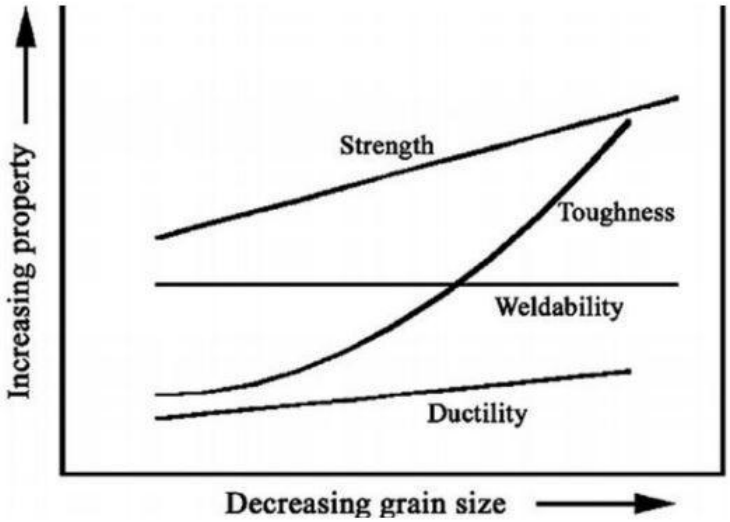


*Figure 2.2 The relationship between decreasing grain size and mechanical properties (Strength, Toughness, Weldability, and Ductility) for metallic compounds [13]*

The Hall-Petch relationship, Figure 2.1, and Figure 2.2 all demonstrate that grain size is inversely proportional to strength. The two point anomalies in Figure 2.1 indicate that severe plastic deformation processing has the ability to preserve metallic ductility. This is because the processing technique induces tremendous amounts of point and line defects in the material, and these defects lead to further microstructure refinement via accelerated atomic diffusion and grain boundary dislocations [14]. These increases in mobile dislocations further enhance the ductility of the UFG materials processed via severe plastic deformation at room temperature by promoting grain boundary sliding (GBS). As the material is subjected to high stress, the dislocations which accumulated at grain boundaries are able to resist necking due to activated GBS [15].

Ultimately, this means the material can maintain ductility when subjected to strain, while demonstrating enhanced strength. The combination of both of these properties can be seen in Figure 2.2, where decreasing grain size is associated with increasing toughness.

## 2.2 Severe Plastic Deformation

Severe plastic deformation techniques are of particular interest to those wishing to develop bulk ultrafine grained materials with attractive mechanical properties. Severe plastic deformation includes all processes which reduce the average grain size of materials through the application of severe stress under hydrostatic pressure [4,5]. This pressure would otherwise cause some overflow in the processing setup, however fixtures generally prevent this change in geometry and keep the volume of the materials reasonably constant.

One such process is High Pressure Torsion (HPT) [12] and it is deemed one of the best processes of creating ultrafine grained materials [16]. HPT is also incredibly effective at achieving the desirable nano-scale grain sizes of 10-100 nm [5,17].

High-Pressure Torsion processing involves a pair of two large anvils which subject a sample to both compressive pressure and torsional strain. While the details of HPT will be discussed in the next section, it is important to discuss the relationship between the number of rotations, $N$, and the increase in strength.

One can see that Al- 7% Si has a higher yield strength and ductility when subjected to HPT. The number of rotations, $N$, is critical to decide the level of grain refinement which might

lead to the desired mechanical properties [18,19]. This study suggests that the number of rotations under compressive loading, *N*, is directly proportional to an increase in strength and ductility [20, 21]. As the sample is subjected to more rotations, and hence more strain, the level of severe plastic deformation occurring in the material increases.

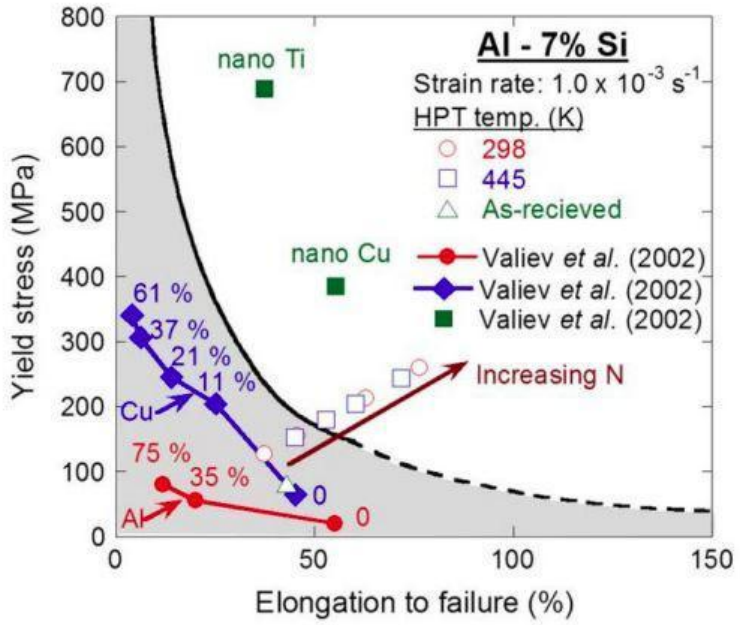


*Figure 2.3 HPT processing of Al-7% Si at 298 K: the red arrow indicates that the number of turns in HPT (N) is proportional to increases in strength and ductility [20, 21]*

## 2.3 High-Pressure Torsion

The technique of High-Pressure Torsion (HPT) was pioneered by Prof. Percy W. Bridgman in 1935 [22]. Bridgman invented HPT as a means to subject materials to extreme torsional shearing stress while under incredible compressive loads, and his research was not limited to only metallic compounds. Some of the materials he processed via HPT included, “pure elements, metallic materials, glasses, geological materials, biological materials, polymers and many different kinds of organic and inorganic compounds” [23] HPT has gained footing in the past three decades, as the need for ultrafine-grained materials has driven research needs and market demands [24].

High-Pressure Torsion loads the sample disk under extreme compressive hydrostatic pressure via two anvils as shown in Fig. 2.4 [25]. One of the anvils rotates at a constant speed,

enabling the material to see both torsional and compressive strains. HPT is successful at achieving true nano-scale microstructures of 10-100 nm under ideal processing conditions.

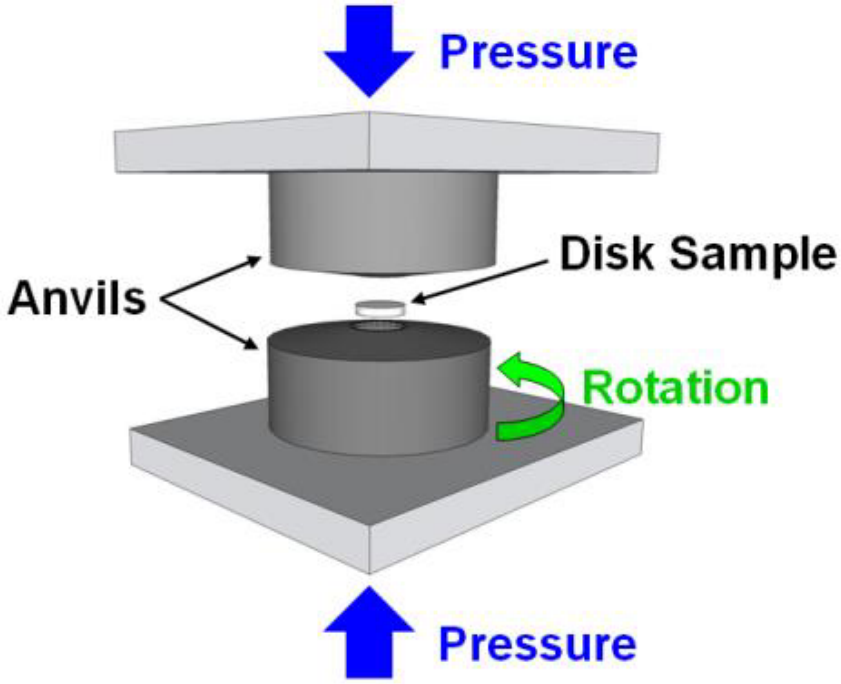


*Figure 2.4 High Pressure Torsion processing of a disk sample with Pressure, P, and rotation of the anvils [25]*

While the concept of hydrostatic pressure and anvil rotation is the same across all forms of HPT, there are three main anvil set-ups. These can be seen in Figure 2.5; these setups all cause different volumes of sample to overflow during testing [16]. The unconstrained (Figure 2.5 a) method results in significant overflow of material, as the sample is not held during compression. Excess volume is able to flow out of the sample bed, which thins the disk and results in substantial material loss. In order to address this issue, fully constrained methods were developed to limit the amount of material that may escape.

However, the fully constrained die design (Figure 2.5 b) introduces significant friction along the cylindrical wall and sample surface. These two problems, sample overflow and stress, led to the development of the quasi-constrained condition (Figure 2.5 c). This intermediate setup stops significant material outflow while not inhibiting the effects of SPD.

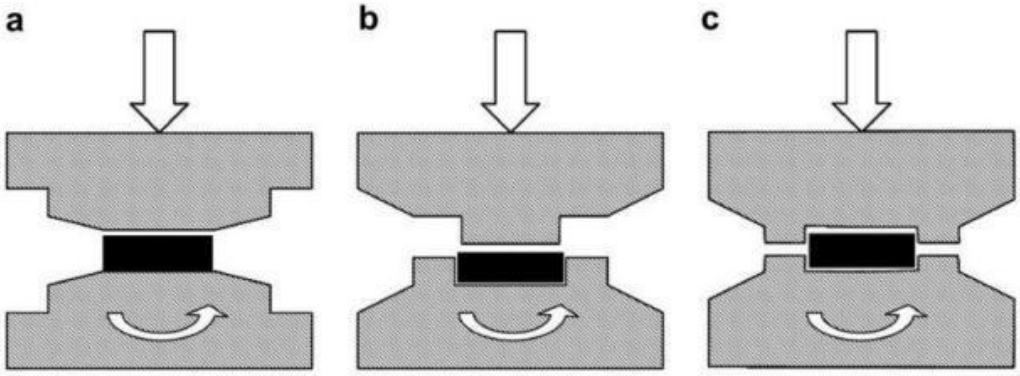


*Figure 2.5 Three different anvil configurations for HPT :*
*a. Unconstrained, b. Constrained, c. Quasi-constrained [16]*

The following equation relates the torsional shear strain, γ, with the number of anvil rotations, *N,* the radial distance from the disk center, $r$, and the height of the disk sample, $h$ [26, 27]. These parameters are also visualized in Figure 2.6 [19].

$$\gamma = \frac{2\pi N r}{h} \qquad \text{Equation 2.2}$$

The distance from the disk center, *r*, is important because the shear strain increases as one gets further away from the disk center. This means that even under constant pressure at a constant rotational speed, the outer diameter of the disk will see more strain than the center. This disk center is theoretically subjected to zero strain, even at any number of rotations, *N*.

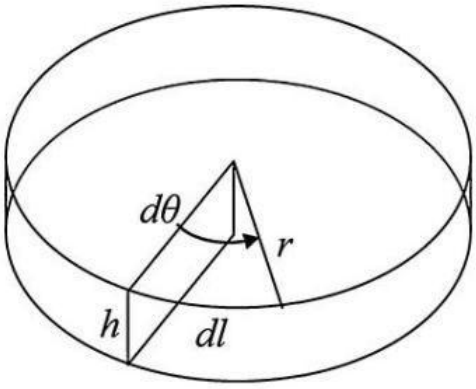


*Figure 2.6 Schematic demonstrating disk height (h) and radius (r) of a typical HPT sample [19]*

The Von Mises equivalent strain, $\varepsilon_{eq}$, (Equation 2.3) indicates that disk height has an inverse relationship with strain [26, 27]. The relationship also backs up the notion that the outer diameter of the disk sees more strain during processing, as the distance from the disk center is at a maximum.

$$\varepsilon_{eq} = \frac{2\pi Nr}{h\sqrt{3}} \qquad \text{Equation 2.3}$$

Both equations 2.3 and 2.2 affirm that the imposed strain is a function of the radius, where equilateral lines of equal stress will occur at the same radial displacement from center. The disk center (where $r = 0$ mm) will experience zero strain and therefore no strain hardening will occur at any numbers of $N$. On the other hand, the maximum strain occurs along the outer edge of the disk, and corresponds to the highest stress that can be seen on the sample [28].

While the value of $N$ also increases the amount of strain within the sample, it is of great interest to investigate how the microstructure and hardness develop during HPT with increasing numbers of $N$. This study examines the changes in both hardness and microstructure of the Al-Li alloy by applying different numbers of HPT turns under constant pressure of 6.0 GPa and a rotational speed of 1 rpm at room temperature.

## 2.4 Aluminum-Lithium Alloys in the Field of Aerospace and Formula Racing

Aluminum alloys are ideal for aerospace and formula racing conditions, as they have low density, high corrosion resistance, superior damage resistance, and high stiffness. Lithium is known as the least dense metallic element. Thus, the addition of Lithium not only increases the strength and modulus, but also reduces the density, thereby increasing the alloy's strength-to-weight ratio. Because Al-Li alloys have this significant weight advantage, many aerospace and automotive industries are interested in the Al-Li 2xxx series of metals. An example of the machined Al-Li alloy parts which are used for formula racing components can be seen in Fig. 2.7 [29]. Due to the popularity of these Al-Li alloys, there are several handbooks which describe the application, common physical and mechanical properties, processing techniques and mechanical behaviors [30].

*Figure 2.7. Al-2099 Bulk Material for Formula Racing [29]*

Aluminum Lithium 2099 is an alloy which is intended for high-strength applications like motorsport and aerospace. Extrusions made from this material are typically used in formula racing components, dynamically and statically loaded fuselage structures, stiffness-dominated products, and lower wing stringers [30]. Even at elevated temperatures, this material continues to demonstrate enhanced toughness, fatigue resistance, and corrosion resistance as shown in Table 2.4 [29].

*Table 2.1 : Mechanical properties of Al-Li 2099, U.K. Smiths High Performance [29]*

| Alloy / Temper | Round Bar | Long Direction | Long Direction | Long Direction | Traverse Direction | | Traverse Direction |
|---|---|---|---|---|---|---|---|
| | (mm) | Rm in MPa | Rp 0.2 MPa | A5 | Rm in MPa | Rp 0.2 MPa | A5 (%) |
| 2099 T83 | 20 - 84 | 560 min | 520 min | 5% min | | | |
| 2099 T83 | 85 - 160 | 560 min | 520 min | 5% min | 460 min | 360 min | 1.5% min |
| 2099 T8 | 161 - 200 | 500 min | 390 min | 5% min | 420 min | 320 min | 1.5% min |

# 3. Experimental Procedures

## 3.1 Sample Material- Al 2099

The experimental material used in this research is Al-2099 T83. This alloy was provided by a U.K.-based company, Smiths High Performance. The extruded bar was initially 12 inches long with a 1-inch diameter and had been heat-treated in the T83 temper (strain hardened by 3%, then artificially aged) [30]. Al-2099 has the following chemical composition (Table 3.1)

*Table 2.2 : Chemical composition of Aluminum-Lithium 2099 [29]*

| Weight % | Al | Cu | Li | ZN | Mg | Mn | Zr | Ti | Fe | Si | Be | Each | Other |
|---|---|---|---|---|---|---|---|---|---|---|---|---|---|
| Min: | Bal | 2.40 | 1.60 | 0.40 | 0.10 | 0.10 | 0.05 | | | | | | |
| Max: | | 3.00 | 2.00 | 1.00 | 0.50 | 0.50 | 0.12 | 0.10 | 0.07 | 0.05 | 0.0001 | 0.05 | 0.15 |

The laboratory at Oregon State University received the 12-inch-long extruded bar, and then machined billets from the material using a lathe. These billets are around 65-70 mm long with a diameter of 10 mm, as shown in Fig 3.1.1. To create the sample disks, the billets were sliced into twenty disks just over 1 mm thick using an Allied High Performance diamond saw (Figure 3.1.2). The temperature was kept low during this process using coolant. To ensure that the samples were not cut smaller than 1.0 mm, each disk was measured using a digital caliper prior to further processing.

*Figure 3.1.1 Machining billets from the as-received material*

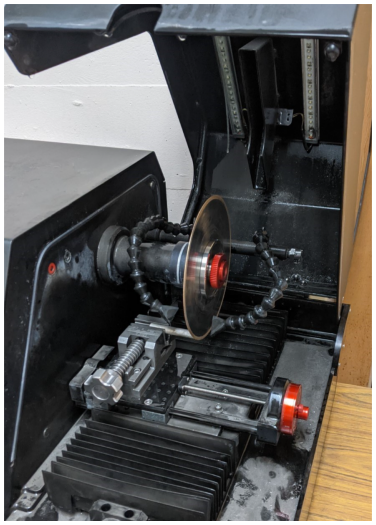

*Figure 3.1.2 Process of cutting disks from the billet inside a diamond saw*

The extrusion, machining, and slicing introduce non-negligible stress to the material, therefore all twenty of the samples were annealed at 600°C for 1 hr. in a Lindberg/Blue induction heating oven. This was done to remove any residual stress in the material.

The disks were then polished down to a final thickness of 0.9 mm on a metallographic grinder. They were polished using silicon carbide papers from Allied Tech Products, Inc. of 200, 800, and 2000 grit. The eight best disks were selected for HPT processing, with diameters of 10 mm and a thickness of approximately 0.85 mm.

## 3.2 High-Pressure Torsion Processing

These disk samples were processed under a semi-constrained HPT System, as can be seen in Figure 2.5(c). Each sample was placed in the depression on the lower anvil before compression. The machine then applied a constant pressure, P, of 6.0 GPa to each sample which caused some material overflow outside the anvil's depression.

While under compression, the bottom anvil rotates at a constant speed of 1 rotation per minute for $N = 1$, 10, and 20 turns at room temperature. The heat produced by this process was monitored to ensure that the temperature would not rise above 70 °C and introduce significant recrystallisation or changes to the microstructure of the material.


*Figure 3.1 HPT System in the Advanced Materials Processing and Analysis Laboratory*

## 3.3 Characterization

After the HPT process, the disks were cut perpendicular to the disk surfaces. After being cast in an epoxy, the cross section and surface of the disks were polished in a consistent manner as described earlier in section 3.2. The polished surfaces are shown in Figure 3.1.

To determine the microhardness values across the cross-section and surface of each sample, the hardness testing machine, a Mitutoyo HM-200 Automatic Harness Testing System (Figure 3.3), was utilized for measuring the hardness values at the different disk measurement regions. At a magnification of 100X, the system took a series of hardness indentations and optical micrographs, stitching them together to generate a complete image. These microhardness arrays were measured using a 100 N load on a rectilinear pattern with a spacing of 0.15 mm. The distance between each sample site is far enough to ensure that local stress caused by each measurement does not affect the surrounding hardness readings.

The surface cross-section (right sample in Figure 3.1) was polished once again. This time, the samples were polished to a mid-surface plane to examine the microstructure by X-ray diffraction (XRD) analysis.

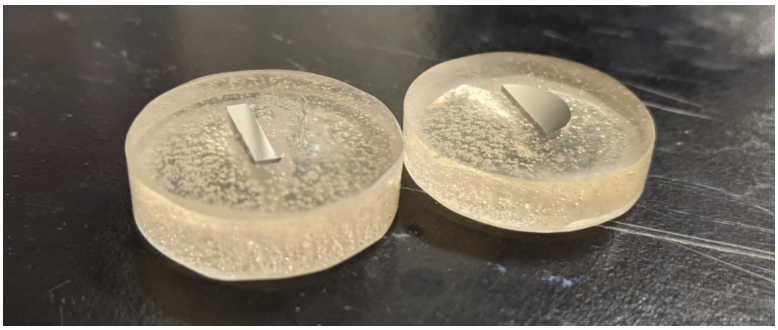

*Figure 3.2 Two epoxy-set samples prior to testing: (left) cross section and (right) surface*

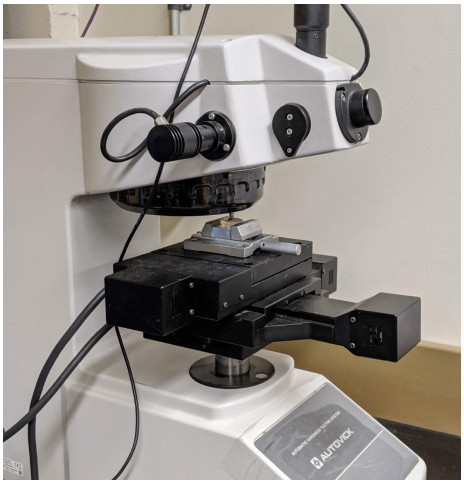

*Figure 3.3 The automatic hardness testing system running a study*

# 4. Results

The microstructure development can be measured using a hardness array. The change in hardness was measured across the 1, 10, and 20 turn samples and plotted as a function of radius. Figures 4.1 and 4.2 demonstrate this change in hardness distribution. Because these samples were processed uniformly, the samples will demonstrate symmetry about the disk center.

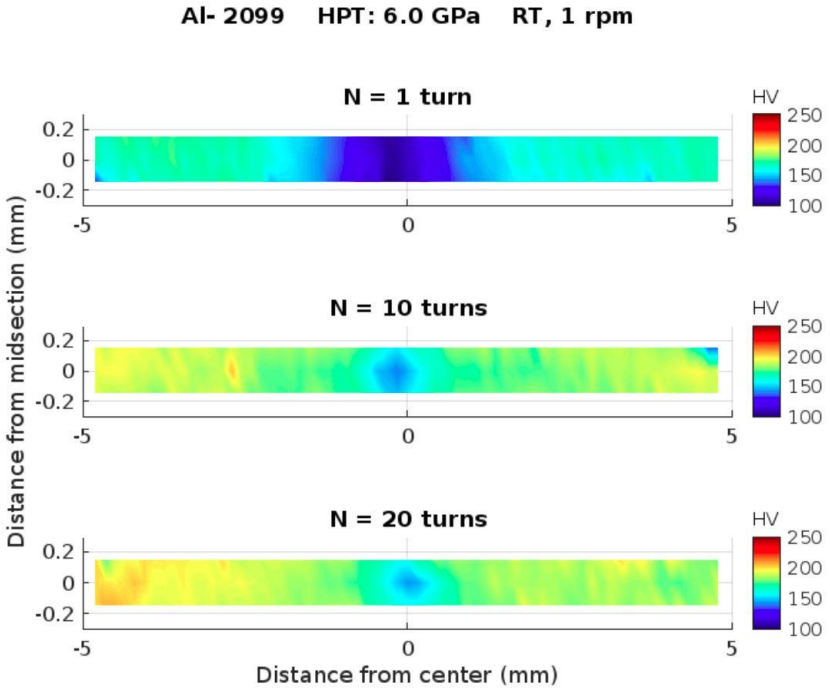


*Figure 4.1 Hardness distribution across the disk cross section*

Even after just one turn under HPT, these disks show a significant change in hardness, from the initial hardness value of 157, to 195 along the disk edge. On the other hand, even after 20 turns, the disk center remains the most ductile. This difference is particularly obvious in Figure 4.1, where the cross section of the disk is plotted over all three testing conditions, $N = 1$, 10, 20 turns.

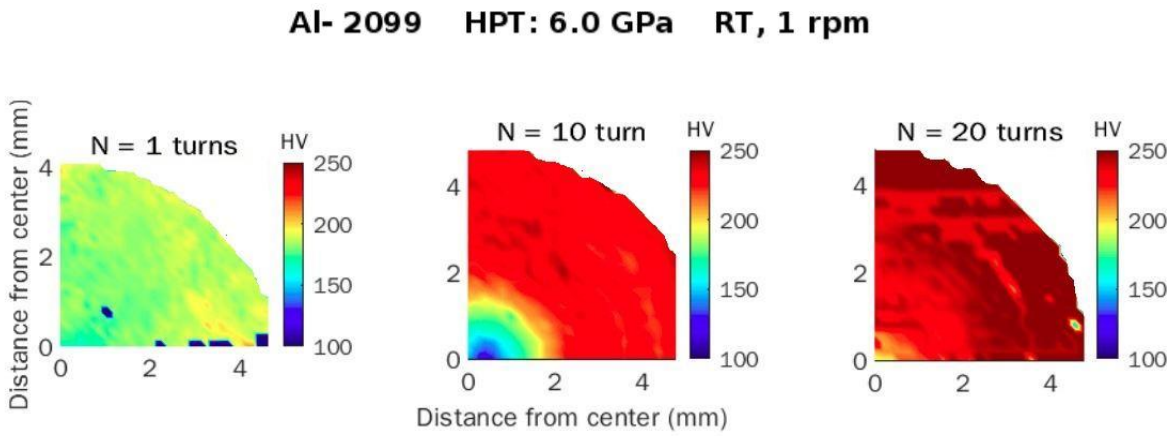


*Figure 4.2 Hardness distributions of the disk surface*

While one turn demonstrates a significant change in the hardness distribution, 10 turns introduces much more strain along the disk edge. A semi-homogenous surface only occurs after 20 turns under HPT, as can be seen in Figure 4.2. The cross section of the disk tells another story, as it's clear that the straining hasn't reached the middle layer of the disk. The surface becomes refined at a faster rate than the vertical cross section.

It is confirmed that 20 turns is enough to refine the surface of the material, however the cross section would require more processing via HPT to achieve homogeneous hardness distributions. It is also confirmed that HPT processing leads to a fine-grained microstructure and enhanced hardness. This microstructure is discussed in the next section, where an XRD of the sample material is discussed.

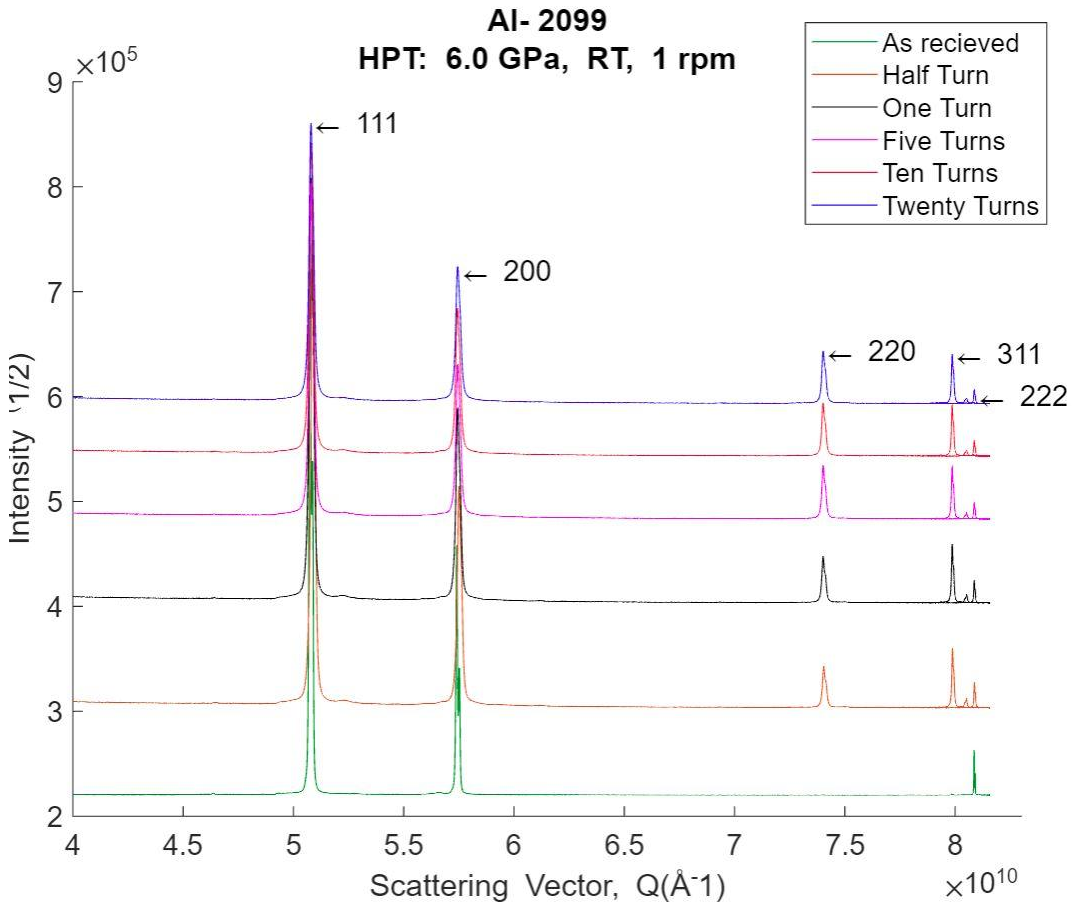


*Figure 4.3 XRD patterns of Al-2099 in as-received and after HPT processing*

The XRD results demonstrate a strong initial texture, with a majority of the alignment along the 111 plane. This occurs because the initial bars were extruded, and the 111 family of planes is the primary mode of slip within the material. As the material gets processed via HPT the material morphs to a weaker texture, with higher quantities of 110, 220, and 311 grain alignment. This occurs because HPT induces deformations along non-111 planes due to the pressure and constrained processing.

# 5. Discussion

In order to determine the hardness development behavior of the Al-Li alloy with grain refinement by HPT processing, the hardness values at the cross-section of the disks as shown in Figure 5.1 were plotted as a function of equivalent strain, $\varepsilon_{eq}$, which is given in Equation 2.3. Not all of the hardness values were used for constructing this plot, but instead the hardness

values at the mid-planes of the disks were applied for consistency. The equivalent strain is a function of both radius and the number of turns, *N*. The radius ranges from $r = 0$ mm - 4.8mm while the number of turns are 1, 10, and 20 turns. A constant disk thickness of $h = 0.8$mm was applied for all specimens. This relationship between the equivalent strain, number of turns, and disk thickness was discussed earlier, and can be seen in Equation 2.3. From this equation, one derives the relationship between hardness developments with equivalent strain by HPT and can therefore determine the hardness development model of the Al-Li alloy.

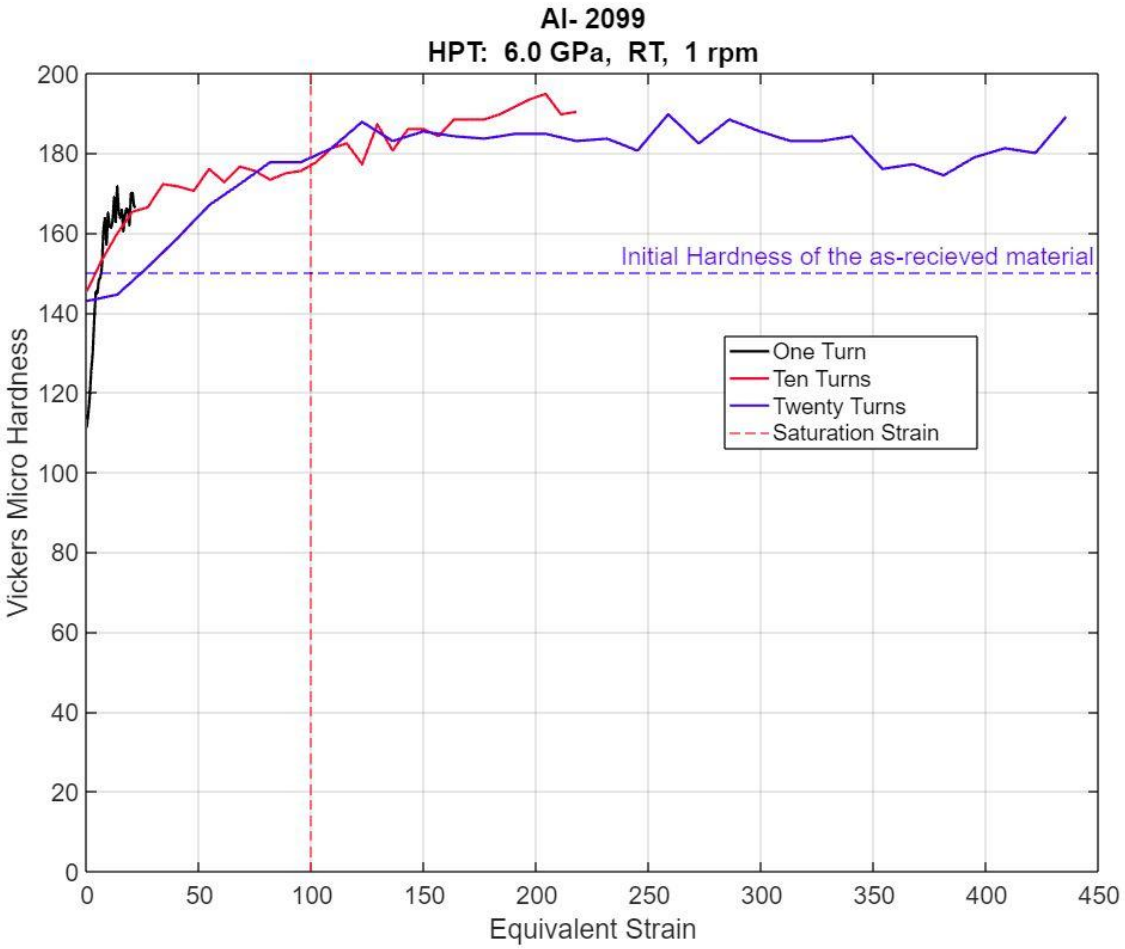


*Figure 5.1 Hardness vs Equivalent Strain for Al-2099 without Recovery*

Figure 5.1 underscores the hardness evolution that occurs as a result of severe plastic deformation. It is apparent that the hardness increases rapidly to a strain of ~50. Strain applied to the material beyond this point, in the ranges of 50-100, further increases the hardness. This

increase is due to the significant grain refinement caused by HPT. This refinement reaches a threshold after the material is subjected to an equivalent strain of 100, where the material cannot be further refined. Beyond this point, the hardness of the material is saturated and any further processing does not provide additional hardness enhancement. Accordingly, severe plastic deformation is an incredibly efficient way to achieve grain refinement, leading to high hardness in Al 2099. An equivalent strain of 100 is necessary to give this material the highest hardness.

This trend of hardness development towards saturation at high hardness following intense grain refinement is a general trend for many common metallic metals and materials, where significant grain refinement occurs with increasing equivalent strain by HPT without any microstructural recovery because of the low enough processing temperature, e.g. room temperature in the present study, in comparison with their melting temperature [31].

XRD results were analyzed by applying the Williamson-Hall analysis. The analysis provides a plot of the full width at half maximum (FWHM), ΔQ, of the diffraction peaks. These widths are plotted against the scattering vector, Q, as shown in Figure 5.2.

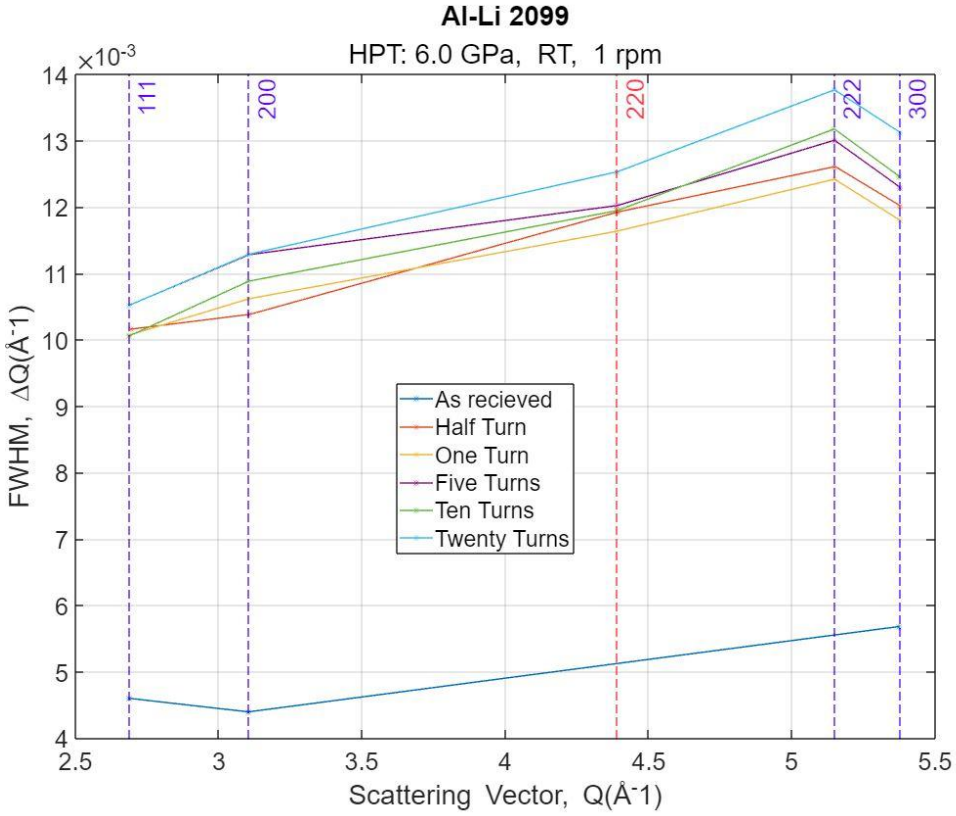


*Figure 5.2. A Williamson-Hall Analysis for Al-2099 HPT Processing*

From this plot, Equation 5.1 describes the positive relationship between the scattering vector and the Full- width at half maximum (FWHM). When plotted as a line, Equation 5.1 gives us the microstrain and average crystallite size in the material. This is useful for determining the change in texture within the material as a result of HPT. Here, the y-intercept ($K\frac{2\Pi}{d_{XRD}}$) determines the crystallite size, whereas the microstrain can be obtained via Δε.

$$\Delta Q = K\frac{2\Pi}{d_{XRD}} + \Delta\varepsilon\, Q \qquad \textit{Equation 5.1}$$

When the y-intercepts and the slopes of each HPT condition are plotted as a function of HPT turns, N, we are able to determine how the crystallite size and microstrain change from the as-received material and through each testing condition. This is vital in understanding the microstructural evolution that occurs during processing.

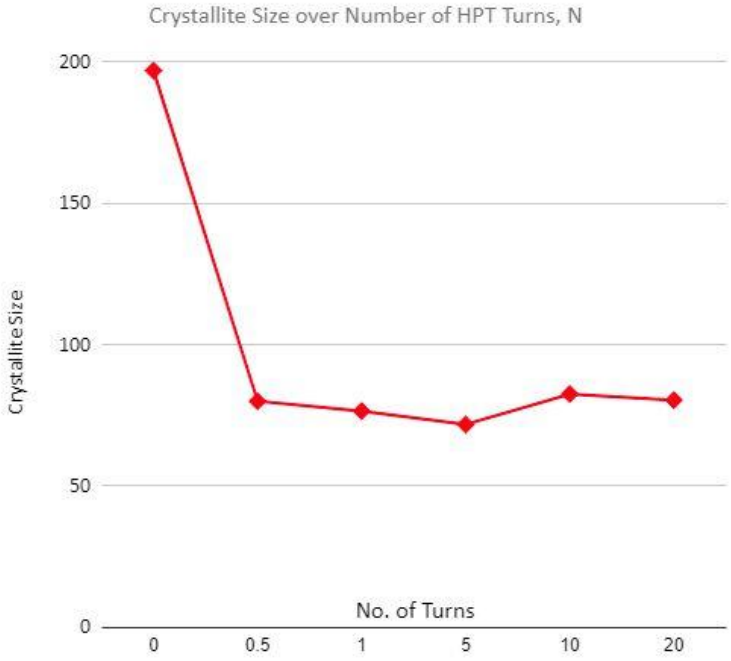


*Figure 5.3: Crystallite (nm) size in Al-2099 as a function of HPT Turns, N*

It is apparent in Figures 5.3 and 5.4 that crystallite size rapidly decreases over ½ turn and reaches a constant grain size after 1-5 turns of HPT. This steady-state crystallite size occurs because of the saturation in the material. These results underscore the results of the strain

analysis: saturation of both the crystallite size and hardness will occur after around 1-5 turns of HPT.

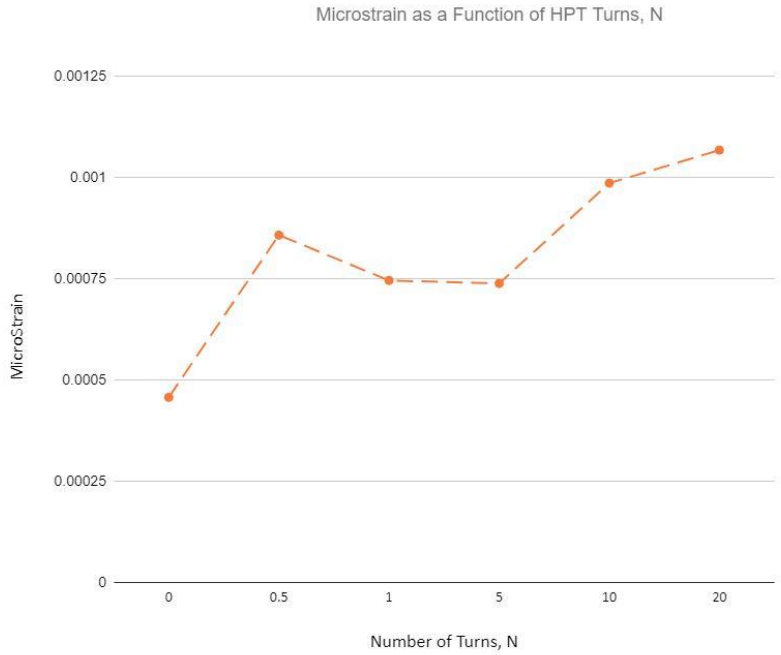


*Figure 5.4 Microstrain in Al-2099 as a function of HPT Turns, N*

Further analysis of the material's microstrain evolution indicates that the material will have a slight increase in the microstrain even after an application of 10 turns. That being said, the majority of the microstrain in the material occurs during the first ½ turn of HPT. This validates the understanding that a small amount of HPT processing is able to drastically change the microstructure of the material.

# 6. Summary and Conclusions

1) Al-2099 was successfully processed via HPT under 6.0 GPa, at room temperature, for up to 20 turns. The initial value was 154 on a Vickers microhardness scale and increased up to a maximum of 241 at the disk edge after 10 turns. This hardness development was consistent throughout 20 turns. Even a small number of turns resulted in significant grain refinement across the disk surface and cross section.
2) The hardness development and equivalent strain analysis demonstrate that the material will become saturated after an applied strain of around 100. After this threshold, the grain

size cannot be refined further even though higher numbers of HPT turns might be applied to the material, Al-Li.

3) The XRD peak profile shows that the as-received material had a strong texture. Because the material had been extruded prior to testing, the as-received material had a very large initial 111 peak. After 20 turns, the sample disks demonstrated a more random texture, with an increase in the 200, 221 and 311 planes.
4) The XRD analysis with the Williamson-Hall method provides quantitative information of the change in texture as a result of HPT processing. The analysis indicates that the microstrain and crystallite size are inversely related.

# 7. Future Work

This study observed the effects of severe plastic deformation on an Al-2099. HPT was already accepted to be a highly effective mode of processing, and the results from this study validate this. However, the grain refinement achieved via HPT is not stable at elevated temperatures. It would be worthwhile to study how the mechanical properties of a processed sample change after heat treatment and time. In order to do this, the samples could be annealed to induce recrystallization and recovery.

Finally, it would be beneficial to compare XRD data in order to see how much the crystallite size changes after both heat treatment and time post-processing.

While the laboratory is limited in tensile testing such a small disk, it would be hugely informative data. The study is currently limited by the grips on the tensile tester, and the fact that a test sample would be less than 5mm x 5mm in size. Future work should involve determining a method by which elongation could be measured to develop a stress-strain response. These tensile test results would be compared with the existing Vickers microhardness values, and any additional nanoindentation studies that are carried out.

# 8. Bibliography


[1] J.W. Martin, Aluminum-lithium alloys, Annu. Rev. Mater. Sci. 18(1) (1988) 101-119.

[2] Sauvage, Xavier, G. Wilde , S.V. Divinski , Z. Horita, R.Z. Valiev, Mater. Sci.Eng. A 540 (2012) 1-12.

[3] M. A. Meyers, A. Mishra, D. J. Benson, Prog. Mater. Sci. 51 (2006) 427-556.

[4] R. Z. Valiev, R. K. Islamgaliev, I. V. Alexandrov, Prog. Mater. Sci. 45 (2000) 103-189.

[5] R. Z. Valiev, Y. Estrin, Z. Horita, T. G. Langdon, M. J. Zehetbauer, Y. T. Zhu, JOM 58 (4) (2000) 33-39.

[6] E. O. Hall, Proc. Phys. Soc. B 64 (1951) 747-753.

[7] N. J. Petch, J. Iron Steel Inst. Jpn. 173 (1953) 25-28.

[8] D. J. Abson, D. J., and J. J. Jonas, Met. Sci. J. 4.1 (1970) 24-28.

[9] T. G. Langdon, Mater. Sci. Eng. A 174 (1994) 225-230.

[10] R. Valiev, Nature 419 (2002) 887-889.

[11] R..Z. Valiev, I..V. Alexandrov, Y..T. Zhu, T..C. Lowe, J. Mater. Res. 17 (2002) 5-8.

[12] A. P. Zhilyaev, T. G. Langdon, Prog. Mater. Sci. 53 (2008) 893-979.

[13] E. Ma, Src. Mater. 49 (2003) 663-668.

[14] S. V. Divinski, J. Ribbe, D. Baither, G. Schmitz, G. Reglitz, H. Rösner, K. Sato, Y. Estrin, G. Wilde, Acta Mater. 57 (2009) 5706-5717.

[15] S. V. Divinski, G. Reglitz, H. Rösner, Y. Estrin, G. Wilde, Acta Mater. 59 (2011) 1974-1985.

[16] A. P. Zhilyaev, T. R. McNelley, T. G. Langdon, J. Mater. Sci. 42 (2007) 1517-1528.

[17] R. Z. Valiev, Y. Estrin, Z. Horita, T. G. Langdon, M. J. Zehetbauer, Y. T. Zhu, JOM 68 (2016) 1216-1226.

[18] A.P. Zhilyaev, S. Lee, G.V. Nurislamova, R.Z. Valiev, T.G. Langdon, Scr. Mater. 44 (2001) 2753.

[19] A.P. Zhilyaev, G.V. Nurislamova, B.K. Kim, M.D. Baró, J.A. Szpunar, T.G. Langdon, Acta Mater. 51 (2003) 753.

[20] T. Mungole, P. Kumar, M. Kawasaki, T.G. Langdon, J. Mater. Sci. 50 (2015) 3549-3561)

[21] P. Kumar, M. Kawasaki, T. G. Langdon, J. Mater. Sci. 51 (2016) 7-18

[22] P.W. Bridgman, J. Appl. Phys. 14 (1943) 273-283

[23] K. Edalati, Z. Horita, Mater. Sci. Eng. A 652 (2016) 325-352

[24] K. Edalati, A. Bachmaier, V.A. Beloshenko, Y. Beygelzimer, V.D. Blank, W.J. Botta, K. Bryła, J.Čížek, S. Divinski, N.A. Enikeev, Y. Estrin, G. Faraji, R.B. Figueiredo, M. Fuji, T. Furuta, T. Grosdidier, J. Gubicza, A. Hohenwarter, Z. Horita, J. Huot, Y. Ikoma, M. Janeček, M. Kawasaki, P. Krăl, S. Kuramoto, T.G. Langdon, D.R. Leiva, V.I. Levitas, A. Mazilkin, M. Mito, H. Miyamoto, T. Nishizaki, R. Pippan, V.V. Popov, E.N. Popova, G. Purcek, O. Renk, Á. Révész, X. Sauvage, H. Sena, V. Sklenicka, W. Skrotzki, B.B. Straumal, S. Suwas, L.S. Toth, N. Tsuji, R.Z. Valiev, G. Wilde, M.J. Zehetbauer, X. Zhu, Mater. Res. Lett. 10 (2022) 163-256.

[25] K. Edalati, Z. Horita, IOP Conf. Ser.: Mater. Sci. Eng. 63 (2014) 012099.

[26] F. Wetscher, A. Vorhauer, R. Stock, A. Pippan, Mater. Sci. Eng. A 387-389 (2004) 809.

[27] F. Wetscher, R. Pippan, S. Sturm, F. Kauffmann, C. Scheu, G. Dehm, Metall. Mater. Trans. A 37A (2006) 1963.

[28] T. G. Langdon, Acta Mater. 61 (2013) 7035-7059

[29] Smiths High Performance, “Aluminum Lithium Alloy”, *www.smithshp.com* (2019) April 24, 2022

[30] N.E. Prasad, A. Gokhale, R. J. H. Wanhill, eds. Aluminum-lithium alloys: processing, properties, and applications. Butterworth-Heinemann, 2013.

[31] M. Kawasaki, J. Mater. Sci. 49 (2014) 18-34